

# REPORT DOCUMENTATION PAGE

AFRL-SR-BL-TR-00-

Public reporting burden for this collection of information is estimated to average 1 hour per response, including the time for review, data needed, and completing and reviewing this collection of information. Send comments regarding this burden estimate or any other aspect of this collection of information, including suggestions for reducing the burden, to Washington Headquarters Services, Directorate for Information Operations and Reports (4302). Respondents should be aware that notwithstanding any other provision of law, no person shall be subject to any penalty for failing to comply with a collection of information if it does not have a valid OMB control number. PLEASE DO NOT RETURN YOUR FORM TO THE ABOVE ADDRESS.

0501

mining the  
reducing  
22202-  
a currently

<b>1. REPORT DATE (DD-MM-YYYY)</b> 05-08-2000		<b>2. REPORT TYPE</b> Final Technical Report		<b>3. DATES COVERED (From - To)</b> 1 Aug 1996 - 31 Jul 1999	
<b>4. TITLE AND SUBTITLE</b> Nonequilibrium Growth of GaN/Si <sub>1-x-y</sub> Ge <sub>x</sub> C <sub>y</sub> /Silicon-on-Insulator				<b>5a. CONTRACT NUMBER</b>	
				<b>5b. GRANT NUMBER</b> F49620-96-1-0339-0399	
				<b>5c. PROGRAM ELEMENT NUMBER</b>	
<b>6. AUTHOR(S)</b> Wilson Ho				<b>5d. PROJECT NUMBER</b>	
				<b>5e. TASK NUMBER</b> 2305/ES	
				<b>5f. WORK UNIT NUMBER</b>	
<b>7. PERFORMING ORGANIZATION NAME(S) AND ADDRESS(ES)</b> Cornell University Office of Sponsored Programs 123 Day Hall Ithaca, NY 14853-2801				<b>8. PERFORMING ORGANIZATION REPORT NUMBER</b>	
<b>9. SPONSORING / MONITORING AGENCY NAME(S) AND ADDRESS(ES)</b> AFOSR/NE Daniel K. Johnstone 801 B, Randolph Street Ph.D. Major, USAF Arlington, VA 22203-1977				<b>10. SPONSOR/MONITOR'S ACRONYM(S)</b> NE	
				<b>11. SPONSOR/MONITOR'S REPORT NUMBER(S)</b>	
<b>12. DISTRIBUTION / AVAILABILITY STATEMENT</b> Unclassified/Unlimited					
<b>13. SUPPLEMENTARY NOTES</b>					
<b>14. ABSTRACT</b> The objectives of this project lies in the growth, characterization, optimization, and fabrication of wide band gap semiconductor thin films and structures. The emphasis lies in the integration of wide band gap semiconductors with silicon and the use of supersonic jet epitaxy to lower the growth temperature and to discover unique and novel applications of this growth technique. Research highlights include the successful growth of silicon carbide, gallium nitride, and aluminum nitride thin films on silicon and miscut silicon substrates, on four-inches silicon wafers, the determination of smooth film-silicon interface and nature of dislocations by cross section scanning transmission electron microscopy, the fabrication of silicon carbide to silicon ohmic contact and rectifying junction with high figures of merit diode properties.					
<b>15. SUBJECT TERMS</b> Wide Band Gap Semiconductors; Supersonic Jet Epitaxy; Low Temperature Growth; Selective Epitaxy; Silicon Substrate; Silicon Carbide; Gallium Nitride; Aluminum Gallium Nitride; Cross Section Scanning Transmission Microscopy; Ohmic Contact; Rectifying Junction; Diode					
<b>16. SECURITY CLASSIFICATION OF:</b>			<b>17. LIMITATION OF ABSTRACT</b>	<b>18. NUMBER OF PAGES</b>	<b>19a. NAME OF RESPONSIBLE PERSON</b>
<b>a. REPORT</b> Unclassified	<b>b. ABSTRACT</b> Unclassified	<b>c. THIS PAGE</b> Unclassified	Unclassified	27	Wilson Ho
			<b>19b. TELEPHONE NUMBER (include area code)</b> (607) 255-3555		

Standard Form 298 (Rev. 8-98)  
Prescribed by ANSI Std. Z39.18

DTIC QUALITY INSPECTED 4

## FINAL TECHNICAL REPORT

### A. Overview

Supersonic jet epitaxy is an intriguing new method for film growth. A directional, high intensity precursor flux can be produced at kinetic energies well above thermal levels. This increase in precursor translational energy helps to overcome the activation barrier for molecular chemisorption. The kinetic energy of the hyperthermal jet can be tuned by using seeding techniques. Heavy molecules mixed in with a light carrier gas are brought to hyperthermal velocities by collisions with the faster-moving light carrier gas during the supersonic expansion process. The precursor molecules accelerated to such energies can enhance dissociative adsorption and increase film growth rates.

Early reactive scattering experiments on metals using supersonic molecular beams revealed that translational energy plays an important role in determining the reactivity of gaseous molecules with surfaces. It is only in the last 10-15 years, however, that hyperthermal molecular beams have been utilized for epitaxial film growth.

The majority of supersonic jet epitaxy studies have thus far been performed on elemental group IV (silicon and germanium) semiconductor growth. The reasons for this are three-fold; suitable substrates exist for homoepitaxial studies, elemental growth represents the easiest system to model, and devices made from silicon, germanium, and their alloys make up the bulk of semiconductor electronics.

A Monte Carlo simulation comparing silicon growth from a thermal (0.17 eV) silicon beam and an energetic silicon beam (5.0 eV) revealed that the kinetic energy of the atomic beam has a dramatic effect on the percentage of crystalline material in the deposit.<sup>1</sup> The simulations show that films grown from energetic beams crystallize at extremely low temperatures (below 175 °C) whereas thermal beams would form amorphous material. Additionally, it was shown that equilibrium surface diffusion did not contribute to atomic rearrangement and that local heating due to atomic energy dissipation was essentially the only source of atomic rearrangement at low temperatures.

---

<sup>1</sup> G. Gilmer and C. Roland, "Simulations of crystal growth: Effects of atomic beam energy", Appl. Phys. Lett. **65**, 824-826 (1994).

Similarly, silicon homoepitaxial growth from thermal and hyperthermal silane ( $\text{SiH}_4$  and  $\text{Si}_2\text{H}_6$ ) precursors has been studied extensively. Both silane<sup>2</sup> and disilane<sup>3</sup> show dramatic increases in reaction probability on clean Si(100) and Si(111) surfaces for energetic beams as compared to thermal beams. Low-temperature epitaxy of group IV semiconductors is limited by the presence of a hydride layer on the growing surface. The activation energy for molecular hydrogen desorption lies between 2 and 2.5 eV, meaning that thermally driven growth can only occur at temperatures above 450 °C. Silicon epitaxy using supersonic (1-2 eV) disilane has been shown to occur at temperatures as low as 400 °C.<sup>4</sup> The excess energy from the hyperthermal silane precursor is transferred locally at the point of impact to the Si-H bonds leading to hydrogen desorption at lower thermal temperatures.

The reaction of germanium hydride molecules on silicon surfaces has shown the same trends as seen for silicon hydride molecules.<sup>5</sup> Again, the reaction probability for these molecules increases with an increase in incident kinetic energy. Epitaxial SiGe has been deposited on Si(001) using hyperthermal silicon and germanium atomic beams. The average silicon and germanium energies were reported as 18 eV and 15 eV, respectively.<sup>6</sup> The experiments showed a substantial increase in critical layer thickness for fully strained  $\text{Si}_{0.7}\text{Ge}_{0.3}$ (001) films as growth temperatures were decreased below 550 °C.

Thermodynamics often works against efficient compound semiconductor growth meaning nonequilibrium growth methods must be relied upon to overcome the associated problems during conventional growth. It is only very recently that studies have been performed on the growth of SiC, GaAs and the III-N semiconductors from supersonic

---

<sup>2</sup> M. E. Jones, L.-Q. Xia, N. Maity, and J. R. Engstrom, "Translationally activated dissociative chemisorption of  $\text{SiH}_4$  on the Si(100) and Si(111) surfaces", Chem. Phys. Lett. **229**, 401-407 (1994).

<sup>3</sup> L.-Q. Xia, M. E. Jones, N. Maity, and J. R. Engstrom, "Dissociation and pyrolysis of  $\text{Si}_2\text{H}_6$  on Si surfaces: The influence of surface structure and adlayer composition", J. Chem. Phys. **103**, 1691-1699 (1995).

<sup>4</sup> R. Malik and E. Gulari, "Pulsed supersonic jet epitaxy: A nonthermal approach to silicon growth", Appl. Phys. Lett. **68**, 3156-3158 (1996).

<sup>5</sup> A. M. Lam, Y.-J. Zheng, and J. R. Engstrom, "Gas-surface reactivity in mixed-crystal systems: the reaction of  $\text{GeH}_4$  and  $\text{Ge}_2\text{H}_6$  on Si surfaces", Surf. Sci. **393**, 205-221 (1997).

<sup>6</sup> N.-E. Lee, N. Matsuoka, M. R. Sardela, Jr., F. Tian, and J. E. Greene, "Growth, microstructure, and strain relaxation in low-temperature epitaxial  $\text{Si}_{1-x}\text{Ge}_x$  alloys deposited on Si(001) from hyperthermal beams", J. Appl. Phys. **80**, 812-821 (1996).

beams. Our own work has shown that the growth rate for both AlN and GaN can be enhanced by increasing the translational energy of the organometallic (TEA, TEG) precursor. At present there are no reports of GaN or AlN growth by chemical beam epitaxy using thermal beams of an organometallic and ammonia. Epitaxial single crystal SiC has been grown by supersonic jet epitaxy in our lab using methylsilane at the lowest reported temperatures to date. We have also directly shown that growth temperatures can be reduced without a change in film characteristics by compensating with an increase in precursor energy. Due to the immensely complicated kinetics involved in heteroepitaxial growth of compound semiconductors, there are no models available as of yet to explain growth using thermal or hyperthermal molecular beams.

## B. Description of Progress

### (i). Research Highlights

- Grew single crystal films of SiC, GaN, and AlN on silicon.
- Demonstrated enhanced growth rate and film quality with increased kinetic energy of the precursors.
- Successfully coupled x-ray scattering from Cornell High Energy Synchrotron Source (CHESS) to monitor film growth.
- Demonstrated importance of initial nucleation on film quality.
- Improved film qualities with growth on miscut silicon substrates.
- Grew single crystal thin films on 4" silicon wafer.
- Extensive cross section scanning transmission electron microscopy studies reveal smoothness of film-silicon interface and nature of dislocations in films.
- Films are optically transparent.
- Ohmic contacts successfully made to SiC on silicon.
- Fabricated n-SiC/p-Si rectifying junction with sharp turn on and low leakage current.

The growth chamber for small area films houses four orifice nozzles capable of providing supersonic jets. Ternary alloys, heterostructures, and n- and p- type doping can all be achieved without removing the substrate from the growth chamber. The large area growth chamber currently houses four tapered slit nozzles and two orifice nozzles. One can control flux uniformity over a 4" diameter silicon substrate by appropriate arrangement of nozzles.

(ii). Supersonic Jet Epitaxy of SiC and GaN in the Small Area Growth Chamber

Thin films of  $\beta$ -SiC(111),  $\beta$ -SiC(002), h-GaN(0002) and  $\beta$ -GaN(002) have been grown on Si(111) and Si(001) using gaseous precursors seeded in  $H_2$ , He, and  $N_2$ . Silicon substrates are cleaned in-vacuo and transferred into a UHV growth chamber for deposition. Growth pressures remain below  $4 \times 10^{-5}$  Torr during all growth runs. Single source organosilicon precursors methylsilane [ $H_3SiCH_3$ ], t-butyldimethylsilane [ $(CH_3)_3CSiH(CH_3)_2$ ], ethyldimethylsilane [ $CH_3CH_2SiH(CH_3)_2$ ], and isopropyldimethylsilane [ $(CH_3)_2CHSiH(CH_3)_2$ ] were all found to produce single crystal SiC films on silicon at temperatures below 1000 °C as indicated by x-ray diffraction (papers 5,6,8,9, and 11 present results from using these precursors). Triethylgallium [TEG;  $Ga(C_2H_5)_3$ ] and ammonia [ $NH_3$ ] were used as precursors for GaN epitaxy. Methylsilane was found to produce the highest quality SiC films and thus was studied the most extensively. RBS analysis indicates that all SiC films grown from methylsilane in this study consisted of equal concentrations of Si and C, *ie.* they are stoichiometric. This is ascribed to the preformed Si-C bond in the methylsilane molecule. Digermane [ $Ge_2H_6$ ], acetylene [ $C_2H_2$ ], disilane [ $Si_2H_6$ ], and methylsilane were used to grow SiGeC.

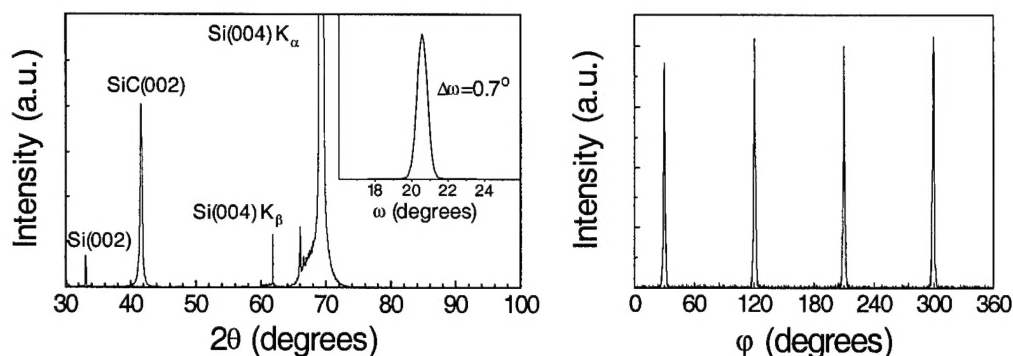


Figure 1. *Left:* X-ray  $\theta$ - $2\theta$  and rocking curve ( $\omega$ ) scans for SiC grown on Si(001) at 700°C. *Right:*  $\phi$ -scan detecting Si{111} peaks. The four fold symmetry indicates a well ordered (001) zinc-blende crystal.

#### a. SiC on Si(001)

On Si(001),  $\beta$ -SiC films were found to form at a temperature of 600 °C, about 100 °C lower than the lowest reported growth temperature for single crystal SiC on silicon to date. XRD from a high quality SiC/Si(001) film (500 nm thick) is shown in Figure 1. Single crystallinity of films is verified by in-plane azimuthal ( $\phi$ -) scans. For a SiC(001) film, the expected four-fold symmetry is observed while scanning SiC{111} planes (Figure 1). A series of films was grown at temperatures between 600 °C and 900 °C using three distinct methylsilane kinetic energies – 0.7 eV, 1.1 eV, and 1.4 eV. At 600 °C and 700°C, an increase in SiC growth rate is seen with an increase in methylsilane translational energy (Figure 2). This enhancement is expected since the methylsilane

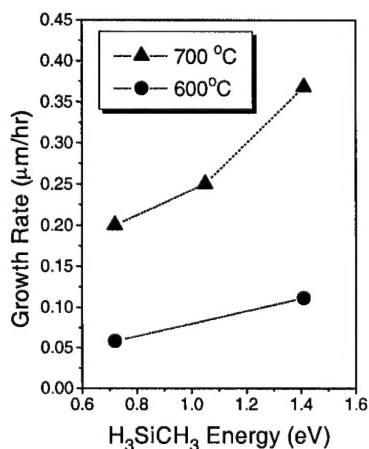


Figure 2. SiC growth rate versus methylsilane translational energy at temperatures of 600 °C and 700 °C. An increase in methylsilane translational energy enhances its chemisorption probability leading to increasing deposition rates.

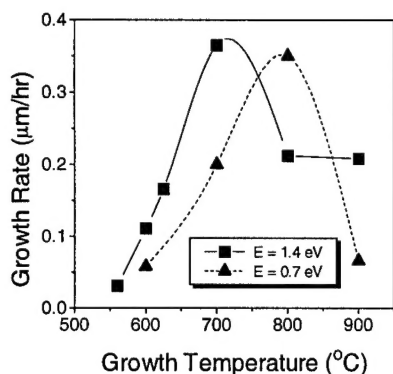


Figure 3. SiC growth rate versus growth temperature for 0.7 and 1.4 eV methylsilane beams. Growth rates increase up to a 'transition' temperature and then drop off sharply.

molecule has been shown to directly dissociate on the SiC surface at hyperthermal energies.<sup>7</sup> It is expected that a further increase in translational energy will continue to improve the growth rate. The growth rate was found to be very sensitive to growth temperature as seen in Figure 3. A dramatic increase in growth rate is observed up to a 'transition' temperature, which varies as a function of methylsilane energy. Beyond the 'transition' temperature, a sharp drop in growth rate is observed. This sharp drop is correlated to a change towards three-dimensional growth and a corresponding increase in surface roughness.  $2\theta$  and rocking curve peak widths follow the same trend as seen for the growth rate, where an improvement in structural order (reduction in peak width) is seen as temperature is increased up to a 'transition' temperature and then a degradation is seen at greater temperatures. The narrowest rocking curve width measured thus far (0.7°) was for a film grown at 700 °C using a 1.4 eV methylsilane jet. It is apparent from Figure 3 that the curve shifts towards lower temperatures for the higher energy methylsilane jet. This is clear evidence that growth with a supersonically expanded precursor can lower growth temperatures by compensating with an increase in precursor translational energy.

Cross-sectional TEM (XTEM) was used to image the SiC/Si(001) interface for a film grown at 800 °C with a 1.4 eV methylsilane beam. Figure 4(a) shows a typical selected area electron diffraction (SAED) pattern taken from a  $\langle 110 \rangle$  cross-sectional sample of the SiC film. The sharpness and symmetrical intensity of the SiC diffraction

compare  
0.2° CVD  
on SiC,  
0.37° MBEVD  
on Si (3C SiC),  
0.18° CVD,  
on SiC, 3C-SiC,  
0.34° LP-RTVD  
on Si & SiC,  
0.31° CVD  
on SiC unibond

<sup>7</sup> L.-Q. Xia, M. E. Jones, N. Maity, and J. R. Engstrom, "Supersonic molecular beam scattering as a probe of thin film deposition processes", J. Vac. Sci. Technol. A 13, 2651-2664 (1995).

spots demonstrate the homogeneous strain distribution within the film. A high magnification STEM image of SiC/Si(001) interface is presented in Figure 4(b). The structural defects within the SiC film are predominantly stacking faults and microtwins. These planar defects are usually observed to lie on {111} planes and terminate within the film as a result of intersecting with each other. They primarily originate from the interface and the density decreases with the distance from the interface. It is important to note that voids were not spotted at any interface examined by XTEM. It is well known that voids occur at the SiC/Si interface due to silicon out-diffusion when carbon reacts at the surface.<sup>8,9</sup> SiC growth from separate silicon and carbon precursors and single source precursors without the correct Si/C stoichiometry will produce voids. Methylsilane chemisorbs with a preformed Si-C bond and thus deters silicon from diffusing and reacting at the interface. This is of major import when considering SiC/Si structures for electronic devices. Figure 4(c) represents an atomic resolution image taken within this region. It reveals the abrupt nature of SiC/Si interface. No planar defects are observed within this region. The continuity of the {111} planes across the interface is visible in this image. Every five SiC{111} planes are registered with four Si(111) planes. The extra lattice fringes can be identified as misfit dislocations. This 'supercell' arrangement reduces the strain at the SiC/Si interface and allows SiC to grow epitaxially in spite of its 20% lattice mismatch to silicon. A schematic model shown in Figure 4(d) illustrates the formation of an array of misfit dislocations when 3C-SiC is grown on Si(001). It has been shown that these misfit dislocations are the pure edge type, which are formed by the interaction of two 60° type of misfit dislocations. They are sufficient to relieve the large lattice mismatch between SiC and Si.

Two SiC films have been grown on 4°-miscut Si(001) substrates. In both cases, films showed improved structural order and smoother surfaces than films grown under

---

<sup>8</sup> J. P. Li and A. J. Steckl, "Nucleation and void mechanisms in SiC thin film growth on Si by carbonization", J. Electrochem. Soc. **142**, 634-641 (1995).

<sup>9</sup> N. Sonoda, Y. Watari, Y. Sun, and T. Mitasato, "Observation of formation processes of hollow voids at the interface between SiC film and Si substrate", Jap. J. Appl. Phys. **35**, L1655-L1657 (1996).



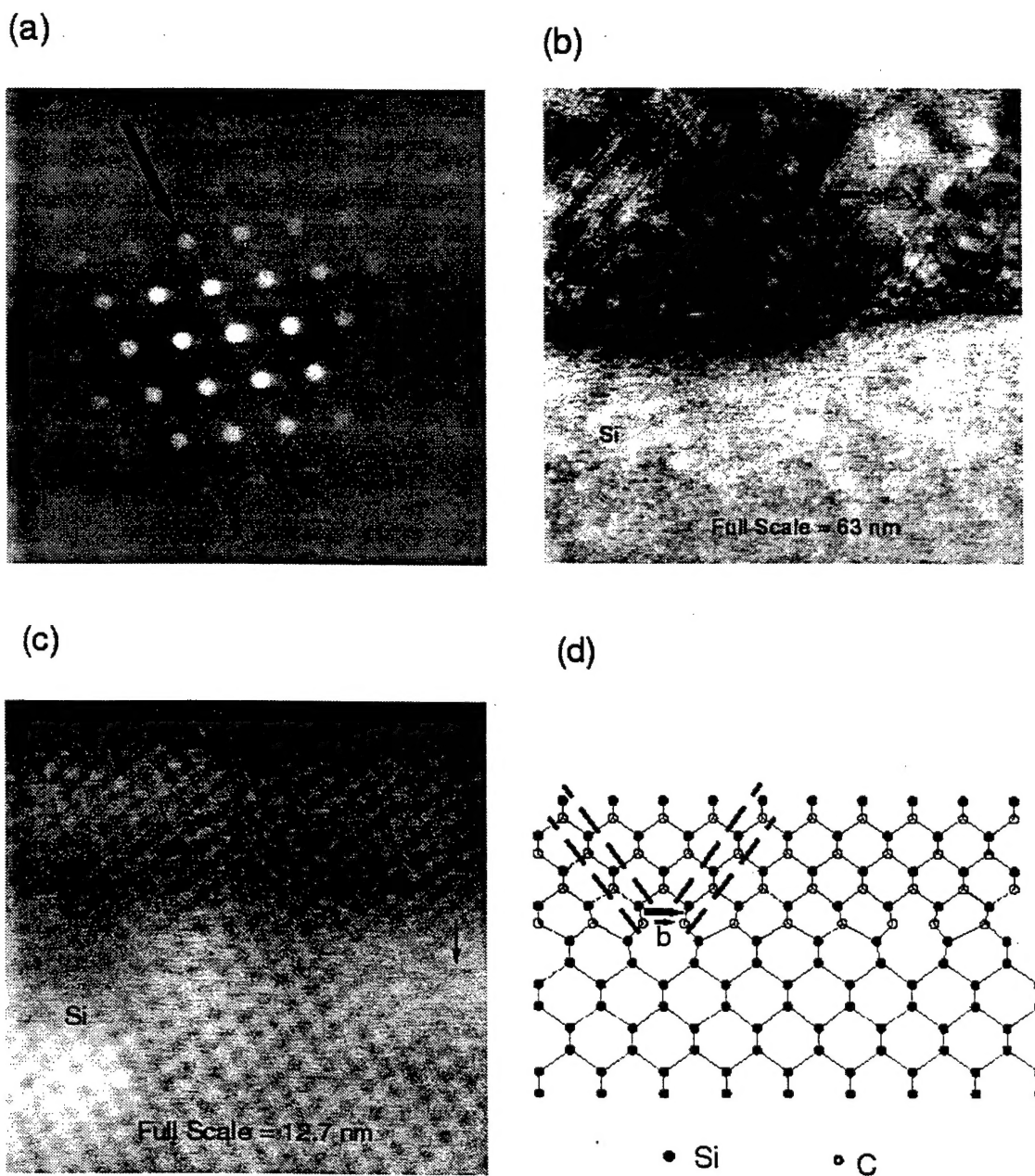


Figure 4. (a) Selected area diffraction pattern (SAED) for  $\beta$ -SiC taken along the  $\langle 110 \rangle$  beam axis. (b) High magnification image of the SiC/Si interface. A stacking fault (SF) in the SiC film is marked. No voids are observed at the interface. (c) Atomic resolution image of the SiC/Si interface. Five SiC{111} planes are registered with four Si{111} planes. Arrows represent the extra SiC{111} planes at the interface. (d) Schematic of an edge dislocation at the interface and its Burgers vector.

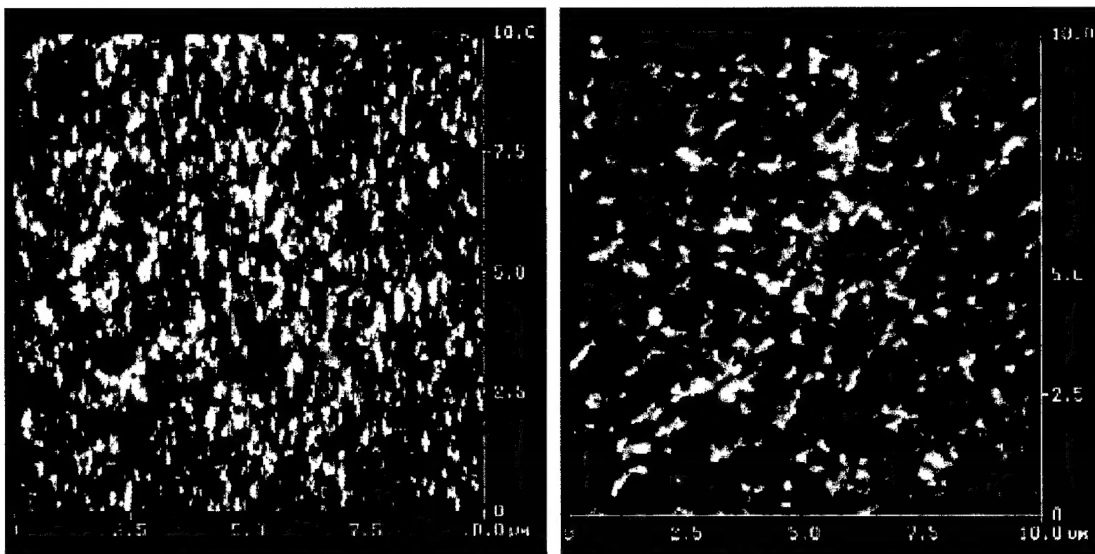


Figure 5. *Left:* AFM image of a 600 nm thick SiC film on Si(001). RMS roughness is calculated to be 26 nm. *Right:* AFM image of 600 nm thick film on 4°-miscut Si(001). RMS roughness drops to 15 nm. Each image is 10  $\mu\text{m}$  square.

the same conditions on on-axis Si(001). Comparative AFM images from films grown on miscut and on-axis Si(001) are shown in Figure 5.

#### *b. SiC on Si(111)*

Single phase SiC films were grown on Si(111) from 550 °C to 900 °C using a 1.4 eV methylsilane beam. The trend in growth rate and XRD peak width versus temperature is similar to that observed from SiC/Si(001) films, the only difference being the ‘transition’ temperature was found to be 800 °C instead of 700 °C. This is not surprising since reactions on (001) and (111) surfaces are quite different, especially at elevated temperatures where surface reconstruction is realized.

Rocking curves indicate a single crystal film but azimuthal scans show otherwise. A zinc-blende (111) film is expected to show a three-fold symmetry about its growth axis, as observed for silicon. Epitaxial SiC(111), however, always shows a six-fold

symmetry,<sup>10,11</sup> as seen in the  $\phi$ -scan shown in Figure 6. Peaks from domains in the SiC film aligned with the Si(111) substrate and those from domains where a stacking degeneracy has occurred are indistinguishable. This indicates that defects within the SiC film are formed as a result of growth kinetics and are not due to lack of registry with the silicon lattice. Rocking curve widths measured from films on Si(111) are generally larger than from films measured on Si(001) due to this stacking degeneracy.

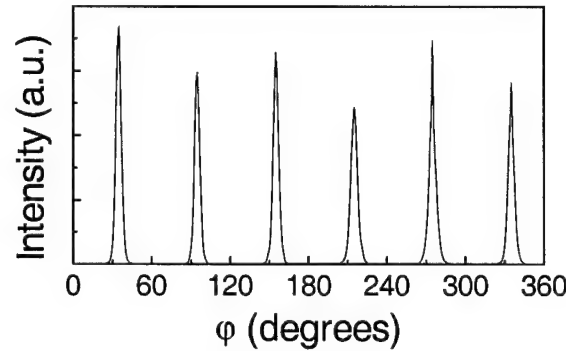


Figure 6. Six-fold symmetry observed for SiC{220} peaks. A three-fold symmetry is expected from a zinc-blende (111) crystal. The extra set of peaks result from regions within the film where twinning has occurred.

A  $\langle 110 \rangle$  axis SAED pattern taken from the SiC/Si(111) interface is presented in Figure 7(a). This film was grown at 900 °C using a 1.4 eV methylsilane beam. The inner set of bright spots is from the silicon substrate. The SiC diffraction pattern consists of two sets of spots due to the twinning process. The diffraction spots from the SiC matrix are aligned with the silicon diffraction spots. The extra diffraction spots are displaced from corresponding diffraction spots from the SiC matrix by  $\pm \left| \frac{1}{3} \langle 111 \rangle \right|$ .

<sup>10</sup> G. L. Zhou, Z. Ma, M. E. Lin, T. C. Shen, L. H. Allen, and H. Morkoç, "Low temperature growth of single-crystalline cubic SiC on Si(111) by solid source molecular beam epitaxy", J. Crystal Growth **134**, 167-173 (1993).

<sup>11</sup> Q. Wahab, R. C. Glass, I. P. Ivanov, J. Birch, J.-E. Sundgren, and M. Willander, "Growth of epitaxial 3C-SiC films on Si(111) silicon substrates at 850 °C by reactive magnetron sputtering", J. Appl. Phys. **74**, 1663-1669 (1993).

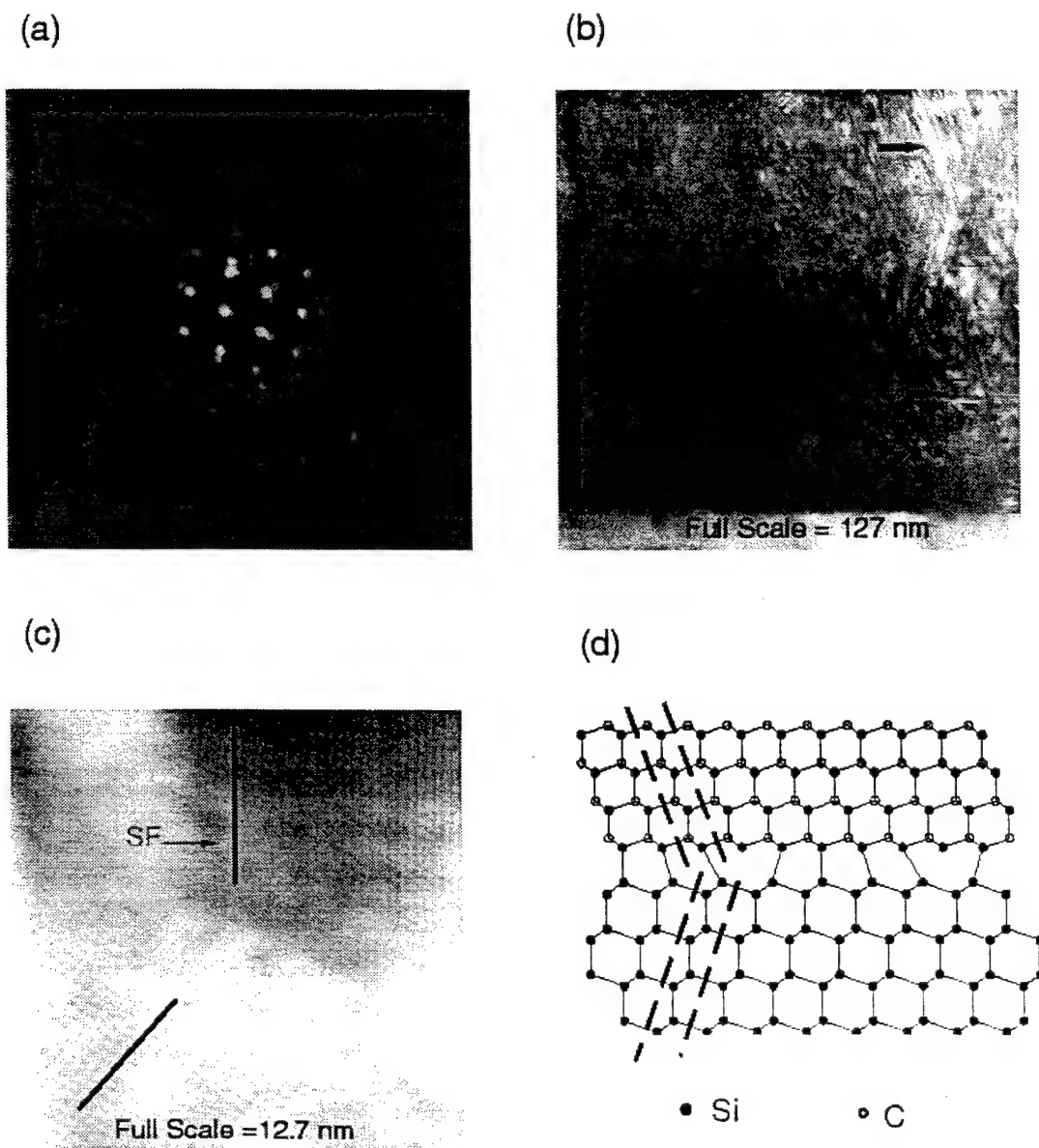


Figure 7. (a) Selected area diffraction pattern from the SiC/Si interface. There are two sets of spots from the SiC film due to twinning. (b) Twins (T) and stacking faults (SF) are observed in the SiC film. (c) Atomic resolution image shows the atomic structure in a twinned region of SiC where the stacking sequence differs from that in the silicon substrate. (d) Schematic of the interface where twinning occurs. The stacking sequence along the  $\langle 111 \rangle$  direction changes from AaBbCcAaBbCc... in the silicon substrate to AaCcBbAaCcBb... in the SiC film.

This feature has been shown to be due to twins.<sup>12</sup> These extra spots are displaced from the matrix reflections in only one  $\langle 111 \rangle$  direction, indicating that twinning occurred on just one  $\{111\}$  plane. The STEM image in Figure 7(b) shows the existence of twins and planar defects within SiC film. Again, no voids are observed at the interface. All the planar defects propagate along  $\{111\}$  planes and are similar to those observed in SiC grown on Si(001). A high resolution micrograph in Figure 7(c) shows the atomic structure of a twinned SiC region. The lattice fringes from twinned SiC( $\bar{1}\bar{1}1$ ) planes are misoriented about  $39^\circ$  from corresponding Si( $\bar{1}\bar{1}1$ ) planes on the  $(1\bar{1}0)$  projection. The  $(1\bar{1}0)$  cross-sectional view of the interface in this micrograph demonstrates the change of stacking sequences in SiC layer across the SiC/Si interface. By using ABCABC... to represent the stacking sequence in Si, the stacking sequence in SiC can be characterized as AaCcBbAaCcBb..., where Aa (or Cc or Bb) represents a Si/C bilayer. Also shown in this micrograph is a stacking fault ending within the twinned SiC region.

SiC(001) and SiC(111) membranes have been produced by back side silicon etching as described previously. A transmission curve through a 500 nm thick film is shown in Figure 8.

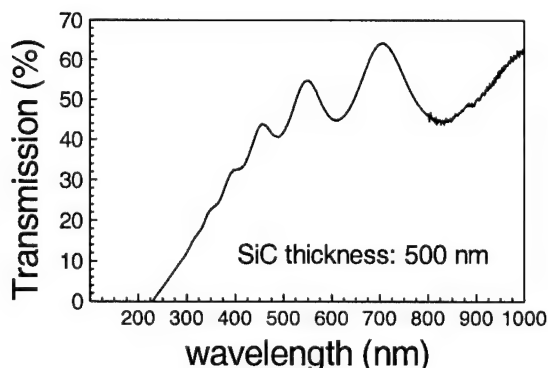


Figure 8. Transmission through a free standing 500 nm thick SiC film. The film is transparent to the eye.

<sup>12</sup> M. J. Stowell, in *Epitaxial Growth Part B*, edited by J. W. Matthews (Academic, New York, 1975), p.460.

### c. Electrical Characterization of $\beta$ -SiC

Electrical characterization of  $\beta$ -SiC films has been carried out. Since silicon substrates are conducting, new characterization techniques were developed to isolate data from the SiC film. Two-layer Hall measurements<sup>13</sup>, where an outer bridge circuit forces the voltage across the SiC/Si junction to zero, have shown the films to be unintentionally *n*-type doped with a carrier concentration of  $1\text{-}2 \times 10^{16} \text{ cm}^{-3}$ . A variety of metals have been employed for ohmic contact to *n*-type SiC. Ni, Ti, Au, Ta and Au/Ti have, after annealing, shown ohmic behavior over several orders of magnitude of current density. We have chosen to use unannealed Al as a contact for electrical characterization since it shows ohmic nature over more than five decades. A contact resistivity of  $\sim 10^{-3} \Omega \cdot \text{cm}^2$  is measured by the circular transmission line model (CTLTM).<sup>14</sup> SiC resistivity was measured and found to be between 0.2 and 0.4  $\Omega \cdot \text{cm}$ . I-V characterization of the  $\beta$ -SiC/Si heterojunction (Figure 9) showed a strongly rectifying junction for unintentionally doped SiC on *p*-type silicon, with a leakage current as low as  $6.6 \times 10^{-4} \text{ A/cm}^2$  at a reverse bias of 10 V. The break down voltage is larger than 40 V. Turn on is rapid at about 0.1 V and the ratio of forward to reverse current at 1 V bias is  $2.2 \times 10^4$ . C-V measurements and I-V measurements as a function of temperature are underway to further characterize the junction. The high quality of the rectifying heterojunction is attributed to a low defect intensity at the interface.

---

<sup>13</sup> R. Larrabee and W. R. Thurber, "Theory and application of a two-layer Hall technique", IEEE Transactions on Electron Devices **27**, p. 32-36 (1988)

<sup>14</sup> G. K. Reeves, "Specific Contact Resistance Using A Circular Transmission Line Model", Solid-State Electron. **23**, 487-490 (1980).

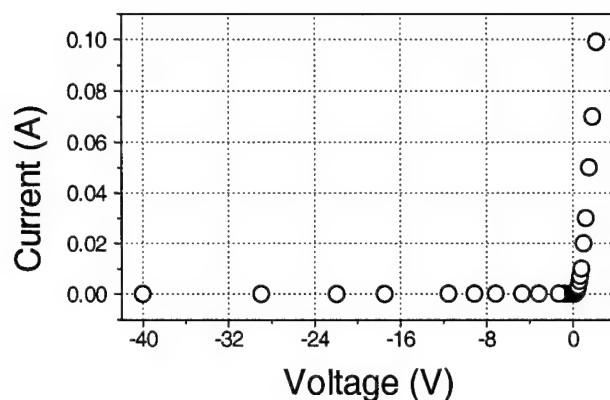


Figure 9. Rectifying n-SiC/p-Si junction using Al as an ohmic contact to SiC.

The breakdown voltage is greater than 40 V. A quick turn on voltage of 0.1 V is measured.

#### *d. GaN on Si(001)*

In order to obtain stoichiometric GaN films, the TEG bubbler needs to be cooled to below  $-17^{\circ}\text{C}$ . Depositing GaN directly on Si(001) normally results in polycrystalline films except under ideal conditions.<sup>15,16</sup> The preference of GaN to form in the wurtzite phase and the large lattice mismatch between silicon and  $\beta$ -GaN combine to make single crystal GaN formation on Si(001) very difficult. Predominantly cubic GaN films have been produced at  $600^{\circ}\text{C}$  and  $700^{\circ}\text{C}$  with broad x-ray features when great care is taken to produce atomically flat Si(001). Deposition of a thin (30 nm) intermediate SiC layer promotes single crystal cubic GaN deposition under stoichiometric or slightly gallium-rich conditions (paper 7). Two series of growths were performed on the SiC/Si(001) system where the translational energy of TEG molecules was varied by changing the seed gas. One series was done at a growth temperature of  $600^{\circ}\text{C}$  and the other at  $700^{\circ}\text{C}$ . In both series a significant increase in growth rate for  $\beta$ -GaN was found as the TEG energy

<sup>15</sup> T. Lei, T. D. Moustakas, R. J. Graham, Y. He, and S. J. Berkowitz, "Epitaxial growth and characterization of zinc-blende gallium nitride on (001) silicon", J. Appl. Phys. **71**, 4933-4943 (1992).

<sup>16</sup> B. Yang, A. Trampert, O. Brandt, B. Jenichen, and K. H. Ploog, "Structural properties of GaN layers on Si(001) grown by plasma-assisted molecular beam epitaxy", J. Appl. Phys. **83**, 3800-3806 (1998).

was increased from 0.4 eV (N<sub>2</sub> seeding) up to 1.8 eV (H<sub>2</sub> seeding) (Table I). In addition, films improved structurally with an increase in temperature for all three energies.

Table I. 2 $\theta$  FWHM, rocking curve ( $\omega$ ) FWHM, and growth rate for GaN/SiC/Si(001) as a function of TEG translational energy and growth temperature.

GaN/SiC/Si(001)									
	GaN 2 $\theta$ FWHM			GaN $\omega$ FWHM			growth rate (nm/hr)		
	H <sub>2</sub>	He	N <sub>2</sub>	H <sub>2</sub>	He	N <sub>2</sub>	H <sub>2</sub>	He	N <sub>2</sub>
600°C	0.96°	0.94°	0.81°	2.5°	2.6°	2.5°	428	428	52.8
700°C	0.58°	0.61°	0.71°	1.5°	1.8°	1.7°	475	475	57.5

Films grown using N<sub>2</sub> as a seed gas showed a much rougher surface morphology (50% greater RMS roughness as calculated by AFM). Surprisingly, little change in x-ray 2 $\theta$  and rocking curve peak widths is observed with the increase in TEG energy. This is in contrast to trends observed in SiC growth, where surface roughening is directly correlated to crystal quality. Based on the breadth of the GaN rocking curves and the increased percentage of defects (as measured by XTEM and XRD) in the GaN films compared to SiC films, we conclude that the roughness of the SiC surface induces three-dimensional nucleation and growth of GaN. In effect, films grown from the highest energy beams were already too rough to show significant structural improvement.

#### *e. GaN on Si(111)*

Since the Si(111) surface is similar to both the h-GaN(0002) and  $\beta$ -GaN(111) surfaces, direct epitaxy of single phase material is difficult. GaN deposited directly on Si(111) has produced single phase wurtzite films under ideal conditions but reproducibility is difficult. Polytypes can be distinguished using x-ray in-plane azimuthal scans. Azimuthal scans searching for  $\beta$ -GaN{220} and h-GaN{10 $\bar{1}$ 1} peaks are performed. Scans detecting  $\beta$ -GaN{220} peaks always show a 6-fold symmetry, similar to scans from SiC(111), although GaN films show varying peak intensity ratios between peaks aligned with silicon peaks and those from the twinned region. Films deposited directly on Si(111) are found to be 95-99% wurtzite phase. Films deposited on 4°-miscut



Si(111) films show a much higher proportion of the cubic phase – about 50%. The greater number of nucleation sites on the miscut surface serve as a template for cubic GaN formation and promote two-dimensional growth (as inferred from lower RMS roughness measured by AFM). When three-dimensional islands form, as on on-axis Si(111), the GaN reverts back to the lower energy wurtzite phase. Films grown on thin (30 nm) SiC(111) intermediate layers showed much improved x-ray characteristics, reducing the GaN rocking curve width down to 0.7°.

XTEM was used to probe a 1  $\mu\text{m}$  thick GaN grown on a 250 nm thick SiC(111) layer. A SAED pattern taken from the GaN film is shown in Figure 10. Although, an azimuthal x-ray scan showed a single wurtzite GaN orientation, the SAED indicates that microscopic misoriented wurtzite inclusions exist within the film. XTEM also shows large undulations at the GaN/SiC interface due to the surface roughness of the SiC film. This rough starting surface promotes defect and dislocation generation in subsequent GaN films.

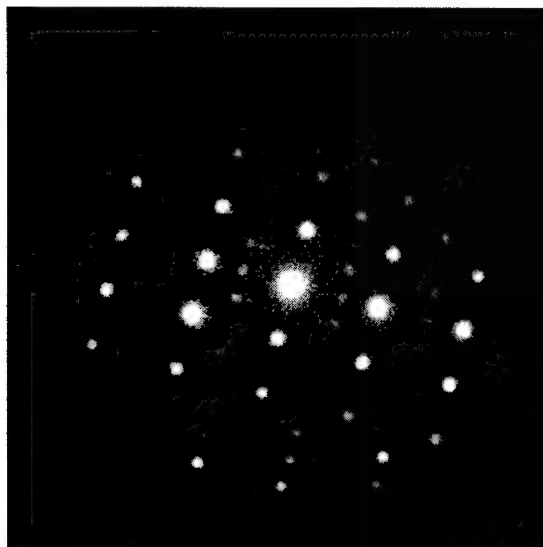


Figure 10. SAED pattern from GaN layer on SiC/Si(111). Spots indicate both wurtzitic and cubic domains exist within the film. The brightest spots correspond to the more predominant wurtzitic phase.

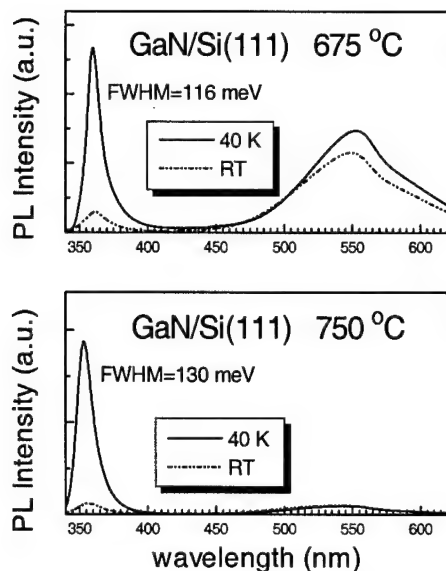


Figure 11. Low temperature (40 K) and room temperature (300 K) photoluminescence from undoped GaN grown on Si(111) at 675 °C and 750 °C. Growth at higher temperatures reduced the generation of gap states that are the source of yellow luminescence.

Low temperature (40 K) and room temperature (300 K) photoluminescence (PL) measurements were carried out on undoped GaN films grown on Si(111) and SiC/Si(001) substrates. Ultraviolet and yellow luminescence was observed from both films with the ultraviolet to yellow peak intensity ratio increasing dramatically at low temperature (Figure 11). GaN/SiC/Si films show only yellow luminescence for films grown at lower temperatures and only very weak UV luminescence appears for films grown at 725 °C.

#### *f. SiGeC*

Attempts were made to deposit SiGeC alloys on silicon by supersonic jet epitaxy. Films were grown using digermene and some combination of disilane, methylsilane, and acetylene. Analysis was performed by Fourier transform infrared absorption and  $\theta$ -2 $\theta$  x-ray diffraction. Auger electron spectroscopy showed Si, Ge, and C on the surface of all films.

Four SiGeC growths were attempted on Si(001) at 700 °C. One experiment used concurrent jets of digermene and methylsilane, the others used pulsed jets. For the concurrent jet growth, a methylsilane to digermene flux ratio of 1 was used. FTIR from this film shows an extremely small peak near 800 cm corresponding to the Si-C stretching mode. Only one peak, attributed to Ge(004), was seen in the XRD spectrum. The methylsilane to digermene flux ratio was raised to 10 and a 125 nm SiC buffer layer

was deposited prior to growth using alternating jets. The XRD spectrum showed peaks from the SiC buffer layer and the subsequent Ge film. Absorbance at  $800\text{ cm}^{-1}$  is evident in the FTIR spectrum as is a peak at  $925\text{ cm}^{-1}$  of unknown origin. It was not possible to continue to raise the ratio of methylsilane to digermane flux due to mass flow controller limitations. To reduce the digermane to methylsilane flux further, a concurrent flow of methylsilane with digermane jet having a 20% duty cycle. Again, FTIR only showed evidence of a Si-C bond at  $800\text{ cm}^{-1}$ . However, XRD showed a  $2\theta$  peak at  $67^\circ$ , instead of at  $66^\circ$  for Ge(004), indicating an alloy with Si and possibly carbon. Reducing the duty cycle of digermane down to 1% did not effect the XRD or FTIR results. These results indicate that, even for low digermane duty cycles, there is too much digermane in the system (and it is too reactive) to allow Si, C, or Si-C incorporation from the methylsilane molecule.

The most promising film produced was grown at  $825^\circ\text{C}$  on Si(001) using an acetylene to digermane ratio of 50. Weak SiC peaks, originating from  $\text{C}_2\text{H}_2$  carbonization of the Si surface, are seen in the FTIR and XRD scans. Strong XRD peaks are seen at  $66^\circ$  and  $31.6^\circ$  corresponding to Ge(004) and Ge(002), respectively. Secondary peaks are seen at  $66.7^\circ$  and  $32.2^\circ$ , which would correspond to the (004) and (002) peaks from a cubic crystal having a lattice constant of  $5.56\text{ \AA}$ . In addition, a small peak in the FTIR absorbance is seen near  $620\text{ cm}^{-1}$  attributed to the localized vibrational mode of substitutional carbon in silicon.<sup>17</sup> These results indicate that a SiGeC alloy with a lattice constant of  $5.56\text{ \AA}$  formed near the film-substrate interface where the silicon was provided by out-diffusion from the substrate. On top of the SiGeC alloy, a pure germanium film was produced when silicon could no longer diffuse through the film.

Two growths were performed on Si(111) at  $825^\circ\text{C}$  using acetylene and digermane. The acetylene to digermane flux ratio was changed from 10 to 100 between growths. A very thin film resulted from the growth at the higher flux ratio (100:1). SiC formation was confirmed by XRD and FTIR. A weak Ge(111) peak was also seen in the XRD scan. On the other hand, the lower flux ratio produced a much thicker film. XRD and FTIR again indicate growth of a thin SiC layer resulting from carbonization. In

---

<sup>17</sup> E. Finkman, H. Rücker, F. Meyer, S. D. Praver, D. Bouchier, J. Boulmer, S. Bodnar, and J. L. Regolini, "Local strains in  $\text{Si}_{1-x-y}\text{Ge}_x\text{C}_y$  alloys as deduced from vibrational frequencies", *Thin Solid Films* **294**, 118-121 (1997).

addition, the XRD spectrum shows a strong double peak at  $27.5^\circ$ . The stronger peak is due to Ge(111) whereas the weaker shoulder peak likely results from the formation of a germanium alloy. No sign of absorption near  $620\text{ cm}^{-1}$  is seen in the FTIR spectrum, however, leading to the conclusion that a SiGe alloy was produced at the interface. One attempt was made to grow SiGeC on Si(111) at  $700^\circ\text{C}$  using methylsilane and digermane. A 125 nm SiC buffer layer was grown and the methylsilane to digermane flux ratio kept at 10. Ge(111) and SiC(111) peaks are observed in the XRD scan and the Si-C and unknown  $925\text{ cm}^{-1}$  peaks are observed in the FTIR scan.

(iii). SiC Growth at CHESS

Preliminary experiments have been performed at the Cornell High Energy Synchrotron Source (CHESS) in order to study the initial nucleation of SiC on Si(001) using a supersonic jet of methylsilane. X-rays are used as a real-time probe for monitoring thickness, surface morphology, and crystal structure. Glancing angle reflectivity is used to study the initial stages of nucleation. Data from one growth at  $800^\circ\text{C}$  is shown in Figure 12. The oscillations observed in the reflectivity are indicative of two-dimensional growth and correspond to a growth rate of  $0.2\text{ }\mu\text{m/hr}$ , comparable to rates observed in our small area growth chamber (see Figure 3) under the similar growth conditions. The damping of the oscillations occurs due to the change from two-dimensional layer-by-layer to three-dimensional cluster growth. This growth mechanism (Stranski-Krastanov) is the most common for heteroepitaxial SiC films. Growth at  $700^\circ\text{C}$  and  $800^\circ\text{C}$  has followed the same pattern during the initial stages – extremely quick nucleation on the silicon surface followed by much slower SiC deposition. Since it appears that methylsilane is very reactive with a silicon surface, it is conjectured that the growing SiC surface is C-terminated.

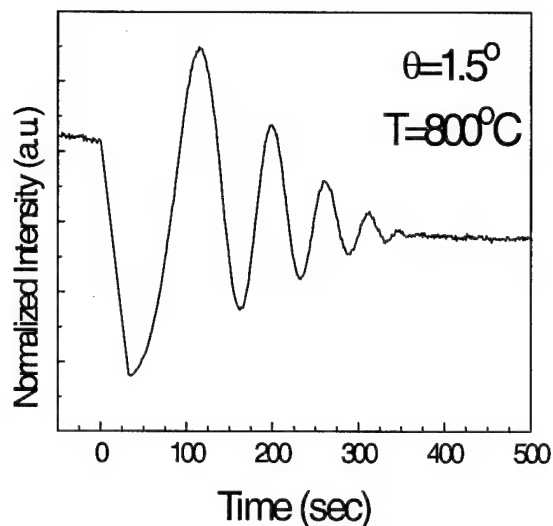


Figure 12. Glancing angle specular x-ray reflectivity recorded during the nucleation of SiC on Si(001) at 800 °C using a 1 eV methylsilane beam. The incident angle is 1.5°.

(iv). Large Area Growth of SiC

Single crystal  $\beta$ -SiC films have been grown on 4" diameter Si(001) substrates in the large area growth chamber using a supersonic jet of methylsilane expanded from a tapered slit nozzle. During growth the chamber pressure rises to 2 mTorr. Films show uniform deposition over approximately 60% of a 4" diameter wafer. A slight reduction in XRD  $2\theta$  and rocking curve peak widths was found with increasing growth temperature. A minimum rocking curve width of  $1.7^\circ$  has been obtained from a  $1\ \mu\text{m}$  thick film grown at 950 °C. The improvement of film quality at elevated temperature is attributed to the enhanced dissociation and mobility of molecules adsorbed on the surface. Figure 13 shows the Arrhenius plot of the growth rate of SiC on Si(001) versus the inverse of temperature. The growth rate in the range of 750 °C to 950 °C varies exponentially with the inverse of temperature. Fitting the data into the general Arrhenius equation  $R = R_0 \exp(-\frac{\Delta H_a}{RT})$ , the apparent activation energy  $\Delta H_a$  is determined to be 1.12 eV/mol from the slope. The is lower than the 2.4 eV/mol activation energy

reported<sup>18,19</sup> from chemical vapor deposition growth of  $\beta$ -SiC on Si(001) by methylsilane. From the linear shape of fitted curve, the growth in this temperature regime is determined to be surface-reaction-limited. This is direct proof that deposition from a supersonically expanded precursor near chemical vapor deposition (mTorr) pressures can lower the thermal activation barrier needed for reaction by compensating with incident translational energy.

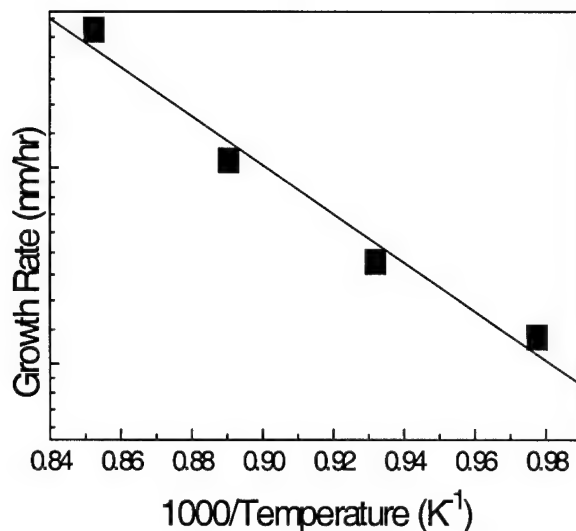


Figure 13. Growth rate versus inverse growth temperature for SiC on Si(001) in the large area growth chamber. An apparent activation energy of 1.12 eV is calculated from the slope.

(v). SiC growth on twist-bonded Si(001)

The epitaxial growth of dislocation-free cubic silicon carbide plays an important role in the fabrication of high power electronics, and attracts much interest and effort. One notorious issue in the development of cubic silicon carbide for device application is the lack of a good substrate. Si substrates offer the potential for integration of state-of-the-art Si technology with SiC-based devices. However the large lattice

<sup>18</sup> A. D. Johnson, J. Perrin, J. A. Mucha, and D. E. Ibbotson, "Chemical vapor deposition of SiC from silacyclobutane and methylsilane", Mat. Res. Soc. Symp. Proc. Vol. **282**, p. 451-456 (1993)

mismatch (20%) between Si and III-V nitrides affects the quality of the epitaxial layers. Y.-H. Lo, *et al.* have grown dislocation-free heteroepitaxial InSb on GaAs substrate by using a compliant universal (CU) substrate<sup>20</sup>. In collaboration with Professor Lo's group, silicon compliant substrates have been made in an attempt to improve the structural quality of highly lattice mismatched films.

When an epitaxial layer is grown on a substrate with a lattice mismatch, the growing layer first elastically distorts itself to fit the crystal matrix up to a critical thickness. At this point, the strain between the substrate and the epitaxial layer is relaxed by generating threading dislocations in the epitaxial layer. These dislocations are detrimental to optical and electronic devices. The goal of the compliant universal substrate is to eliminate the dislocations. Essentially, a compliant universal substrate is a twist-bonded thin layer between the bulk substrate and the epitaxial layer. A network of screw dislocations is formed at the boundary between twisted layer and the bulk substrate. This grid of screw dislocations at the interface accommodates the twist. At the cores of the dislocations the atomic bonds are stretched. The thin layer is elastic rather than rigid because it is sitting on stretched, weakened bonds.

The compliant universal substrate is created by direct wafer bonding applied with a twist angle. In our experiments, the host wafer is bulk Si, and the seed wafer is SIMOX (Separation by IMplantation of OXYgen), which consists of an ultra thin silicon layer (about 50 nm), an etch stop layer (SiO<sub>2</sub>), and bulk Si. The Si compliant substrate is fabricated by the following process: The wafers are ultrasonically cleaned with acetone, methanol, and isopropanol. After a thorough DI water rinse, the surfaces of both wafers are immersed in a diluted HF solution. The two wafers are finally rinsed in DI water, blown with dry nitrogen, and immediately brought into contact with misaligned crystal orientations. If the wafer surfaces are flat and clean, the wafers will be bonded by van der Waals forces as soon as they are in contact. The sample is then clamped into a vise by applying a strong and uniform pressure. The entire holder is loaded into a vacuum furnace. The temperature is ramped from room temperature to 1000 °C with a ramp rate

---

<sup>19</sup> G. Krötz, W. Legner, G. Müller, H. W. Grueninger, L. Smith, B. Leese, A. Jones, and S. Rushworth, "Structural and electronic characterization of  $\beta$ -SiC films on Si grown from mono-methylsilane precursors", *Mat. Sci. and Eng. B* **29**, p. 154-159 (1995).

<sup>20</sup> F. E. Ejeckam, M. L. Seaford, Y.-H. Lo, H. Q. Hou, and B. E. Hammons, "Dislocation-free InSb grown on GaAs compliant universal substrates", *Appl. Phys. Lett.* **71**, 776-778 (1997).

of 5 °C, and maintained at 1000 °C for 30 minutes. The final step of wafer bonding involves removal of the substrate of the seed wafer by mechanical lapping and selective chemical etching. The bulk Si of the SIMOX wafer is first mechanically polished down to 40  $\mu\text{m}$ . The residual Si and SiO<sub>2</sub> are etched away by selective etching in KOH and HF, respectively. The thickness of final compliant Si layer can be further reduced by oxidation and HF etch. In the experiments, the thickness of compliant layer ranges from 10 nm to 20 nm.

Three SiC films have been grown on 45° twist-bonded Si(001) at 700 °C. One substrate (with a 20 nm silicon layer) was pre-cleaned with HF before insertion into vacuum. This sample was cleaned in vacuum by sputtering and annealing at 1000 °C. Theoretical calculations provided the conditions (beam voltage and beam current) for sputter removal of only 100 Å prior to growth. The SiC film grown on this surface was found to form equally in two orientations, one aligned with the twisted silicon lattice and one aligned to the bulk silicon lattice. The other two substrates were protected with a chemical oxide. For these substrates the chemical oxide was desorbed at 925 °C immediately prior to growth. On a 10 nm silicon layer the resulting SiC film was aligned with bulk silicon lattice. On a 20 nm silicon layer the film was oriented aligned to both the bulk silicon and the twisted silicon.

The films grown on all three substrates were of similar quality to those grown directly on Si(001). In all three cases, it does not appear that growth took place on a true CU substrate. The silicon layer in the SIMOX substrates is chemically reduced from an original (reported) thickness of 50 nm. The company that provided the wafer specified the variation in this thickness as 5 nm. We attempted to reduce the thickness from 50 nm to 10-20 nm by chemical oxidation and etching. The amount of material removed is estimated from well-known chemical oxidation and etch rates. It appears, however, that there was too much variation in the original silicon layer to provide a uniform 20 nm twisted layer. Since growth on these substrates resulted in films aligned with both the bulk silicon lattice and the twisted silicon lattice it stands to reason that the original substrate contained regions of both twist-bonded silicon and bulk silicon. Growth on the (estimated) 10 nm twisted layer resulted in a film aligned with the bulk silicon lattice. This could be due to a large variation in silicon thickness from the SIMOX wafer or from the thin layer untwisting during the desorption of the oxide at 925 °C.



(vi). TEM analysis of SiC wafer bonding

Silicon-on-Insulator (SOI) technology has recently been used in the fabrication of low-voltage integrated circuits. Silicon carbide is a promising material for device application due to its extreme electrical properties. An interesting approach to fabricate SiC-based devices is SiC-on-Insulator (SiCOI) technology. In collaboration with Materials and Technologies Corp., a SiC film grown by supersonic jet epitaxy was bonded to SiO<sub>2</sub>. Cross-sectional TEM gives direct proof of the SiC/SiO<sub>2</sub> bonding as shown in Fig. 14. A thin SiC layer (about 8 nm) is sandwiched between Si and SiO<sub>2</sub>. The SiC surface fluctuation estimated from the 500 kX micrograph is about 1 nm. The 5 mX high resolution TEM micrograph shows a uniform SiC/SiO<sub>2</sub> interface in a small region. The surface morphology of SiC is vital to SiC/SiO<sub>2</sub> bonding process. A flat and uniform SiC surface should be optimized to achieve SiC/SiO<sub>2</sub> bonding, and to reduce the defects at the SiC/SiO<sub>2</sub> boundary and the density of interface traps that would be detrimental to the performance of devices.

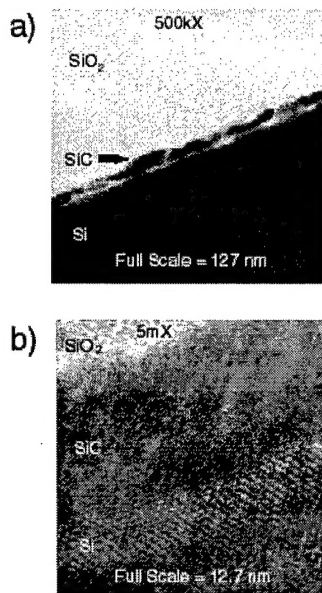


Figure 14. Cross-sectional TEM of SiC wafer bonded to SiO<sub>2</sub>/Si(001).

a) The 500 kX micrograph shows an abrupt SiC/Si interface but some fluctuation at the SiC/SiO<sub>2</sub> bonded interface.

b) The 5 mX micrograph shows a uniform SiC/SiO<sub>2</sub> interface over a small area.

(vii). List of Publications on Wide Band Gap Semiconductors

1. K. A. Brown, S. A. Ustin, L. J. Lauhon, and W. Ho, "Supersonic jet epitaxy of aluminum nitride on Si(100)", J. Appl. Phys. **79**, 7667 (1996).
2. P. E. Norris, L. D. Zhu, H. P. Maruska, W. Ho, S. A. Ustin, and L. J. Lauhon, "Supersonic jet epitaxy: An improved method for nitride deposition", Mat. Res. Soc. Symp. Proc. **395**, 301 (1996).
3. S. A. Ustin, L. Lauhon, K. A. Brown, D. Q. Hu, and W. Ho, "Single crystal wurtzite aluminum nitride growth on silicon using supersonic gas jets", Mat. Res. Soc. Symp. Proc. **395**, 319 (1996).
4. L. J. Lauhon, S. A. Ustin, and W. Ho, "Large area supersonic jet epitaxy of AlN, GaN, and SiC", Mat. Res. Soc. Symp. Proc. **449**, 277 (1997).
5. J.-H. Boo, S. A. Ustin, W. Ho, H. P. Maruska, P. E. Norris, I.-H. Kim, and C. Sung, "Growth of cubic SiC thick films on silicon from single source precursors by supersonic jet epitaxy", Mat. Res. Soc. Symp. Proc. **441**, 705 (1997).
6. J.-H. Boo, S. B. Lee, S. A. Ustin, W. Ho, H. P. Maruska, P. E. Norris, I.-H. Kim, and C. Sung, "Growth of epitaxial cubic SiC thin films using single source precursors", Mat. Sci. Forum **264-8**, 187 (1998).
7. S. A. Ustin and W. Ho, "Single crystal gallium nitride on silicon using SiC as an intermediate layer", Mat. Res. Soc. Symp. Proc. **482**, 313 (1998).
8. S. A. Ustin, C. Long, L. J. Lauhon, and W. Ho, "Single crystal silicon carbide on silicon using a supersonic gas jet of methylsilane", Mat. Res. Soc. Symp. Proc. **483**, 279 (1998).
9. J.-H. Boo, S. A. Ustin, and W. Ho, "Supersonic jet epitaxy of single crystalline SiC thin films on Si substrates from *t*-butyldimethylsilane", Thin Solid Films **324**, 124 (1998).
10. J.-H. Boo, S. A. Ustin, and W. Ho, "Growth of hexagonal GaN thin films on Si(111) with cubic SiC buffer layers", J. Cryst. Growth **189/190**, 183 (1998).
11. S. A. Ustin, C. Long, and W. Ho, "Supersonic jet epitaxy of silicon carbide on silicon using methylsilane", Solid State Electronics **42**, 2221 (1998).
12. J.-H. Boo, S.A. Ustin, and W. Ho, "Low-Temperature Epitaxial Growth of Cubic SiC Thin Films on Si(111) Using Supersonic Molecular Jet of Single Source Precursors", Thin Solid Films **343**, 650 (1999).

13. C. Long, S. A. Ustin, and W. Ho, "*Structural defects in 3C-SiC grown on Si by supersonic jet epitaxy*", J. Appl. Phys. **86**, 2509 (1999).
14. S.A. Ustin, K.A. Brown, and W. Ho, "*An Apparatus for Supersonic Jet Epitaxy of Thin Films*", Rev. Sci. Instrum. **71**, 1479 (2000).